22 Mar 2004

Dynamic Contact Angles under Evaporation

Robert M. Ybarra

Partho Neogi

Missouri University of Science and Technology, neogi@mst.edu

Dynamic contact angles under evaporation

Robert M. Ybarra
Rolla, Missouri 65401

P. Neogi
Chemical Engineering Department, University of Missouri—Rolla, Rolla, Missouri 65409

(Received 30 September 2003; accepted 31 December 2003)

Wetting kinetics in the presence of heat transfer, evaporation, and Marangoni effect has been explored using a method used by Joanny and de Gennes [C. R. Acad. Sci. Ser. II **299**, 279 (1984)]. The method solves for the dynamic contact angle α by equating the rate of surface work to the rate of dissipation. The result in the form of dynamic contact angle α as a function of capillary number Ca agrees well with existing experimental data. Qualitative comparisons have been made in cases where quantitative data do not exist. Finally, a form of contact line instability is predicted, for which some experimental justifications are seen. © *2004 American Institute of Physics.*
[DOI: 10.1063/1.1649932]

INTRODUCTION

When a flat plate is withdrawn (or immersed) from (into) a pool of liquid at a constant velocity U, the angle α that the meniscus makes with the plate is the dynamic contact angle. The relationship between U and α under heat transfer is sought below. Consider Fig. 1(a) where the plate is held at temperature T_w, a temperature greater than the ambient saturated vapor at temperature T_s. The evaporating meniscus depletes the liquid pool in the contact line region; however, the upward movement of the plate at velocity U compensates for this evaporative loss and results in a meniscus with a steady-state configuration. Such phenomena arise in boiling heat transfer.[1,2] In Fig. 1(b), we have sketched a similar problem but one where the ambient fluid at T_∞ represents unsaturated air. In Fig. 1(a) the temperature at the liquid–vapor interface remains constant at T_s, but in Fig. 1(b) this temperature varies along the interface. This temperature variation leads to the Marangoni effect and instability of the contact line. Disturbances at the contact line undergoing heat transfer sometimes display a wavy but steady appearance[3,4] while at other times exhibit a kicking and biting motion.[5]

The detailed transport problem is very difficult to solve,[6] however, Joanny and de Gennes[7] addressed the fluid flow problem by balancing the rate of viscous dissipation with the rate of surface work. For a wetting liquid considered here, a very thin precursor film that cannot be seen in microscopy (but can be under much higher resolution as in ellipsometry) lies ahead of the contact line.[8] Data on such precursor films are not reported in most experiments and its dynamics are not analyzed in most models under the assumption that those in the two regions can be uncoupled as the precursor moves ahead much faster than the bulk liquid. In Fig. 1, the rate of surface work for a wetting liquid is $-U(\gamma\cos\alpha+\gamma_{SL}-\gamma_S)$ where γ, γ_{SL}, and γ_S represent the surface tensions at liquid–vapor, liquid–solid, and solid–vapor interfaces. For small values of α, this rate reduces to $-U(\gamma+\gamma_{SL}-\gamma_S-\gamma\alpha^2/2)=U(S+\gamma\alpha^2/2)$, where the term associated with the spreading coefficient S represents the dissipation in the precursor film. For a wedge shown in Fig. 1 described by the local film thickness $z=h(x)$ (and referred to henceforth as h), the surface work reduces to $U\gamma\alpha^2/2$.

Lubrication theory approximation[9] is used to analyze the transport in the liquid, where film is assumed to be flat and thin. Consequently, the only velocity component considered is v_x and that it is assumed to vary mainly in the z direction. The heat transfer in the x direction is not considered because the small film thickness makes conductive flux in the z direction by far the most important contribution. This signifies that to the first approximation the temperature T varies mainly in the z direction. For the lubrication theory approximation to hold in the presence of the loss of liquid by vaporization, it requires that vaporization be low, both for the film to remain uniformly thin and velocities (characterized by U) to remain low. The rate of dissipation per unit volume for the wedge becomes[10]

$$\phi=\frac{k}{T}\left(\frac{dT}{dz}\right)^2+\mu\left(\frac{dv_x}{dz}\right)^2, \tag{1}$$

where k is the thermal conductivity and μ is the viscosity. In the analysis of similar problems, Shanahan[11,12] has ignored the heat-transfer terms in Eq. (1). Thus the extension of the balance given by Joanny and de Gennes[7] to the wedge undergoing heat transfer becomes

$$\gamma\alpha^2/2=\int_v \phi dV+N, \tag{2}$$

where V represents the total liquid volume. The term N is new. It accounts for the nonisothermal nature of the vapor–liquid interface. The details of N, which includes variations in surface tension with temperature, can be defined when the nature of the boundary value problem is specified.

EVAPORATION INTO SATURATED VAPOR

Under lubrication theory approximation, the momentum balance becomes

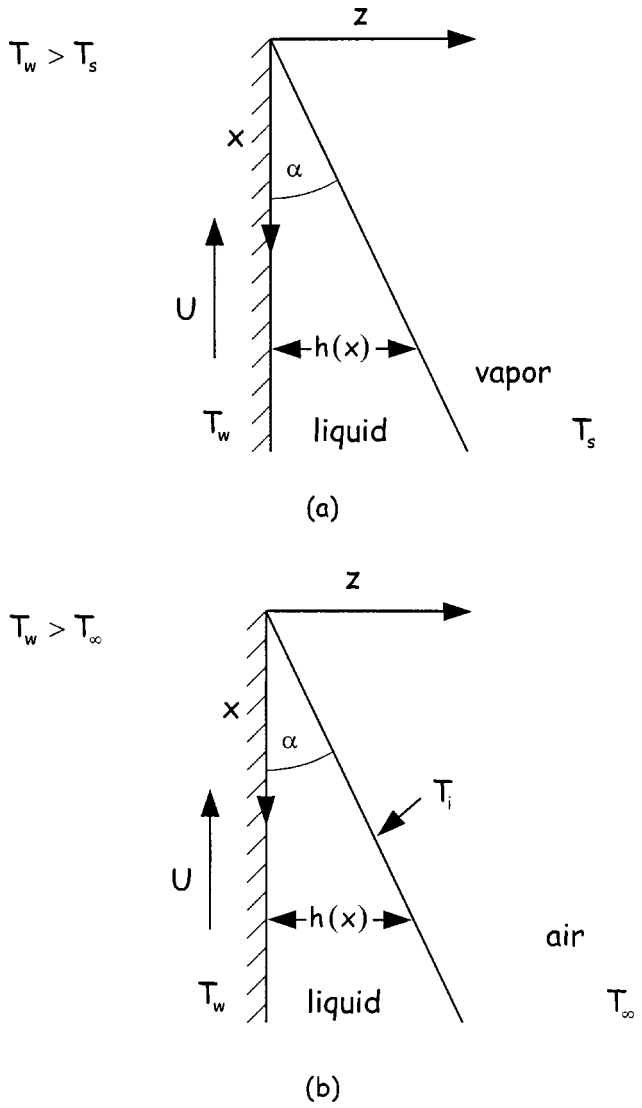

FIG. 1. Schematic views of the contact line region evaporating into (a) saturated vapor and (b) air. Conditions and coordinates are shown.

$$0 = -\frac{\partial \wp}{\partial x} + \mu \frac{\partial^2 v_x}{\partial z^2}, \tag{3}$$

$$0 = -\frac{\partial \wp}{\partial z}, \tag{4}$$

where $\wp$ is the dynamic pressure p-$\rho g x$. Eqs. (3) and (4) are subject to the boundary conditions

$$\left.\frac{\partial v_x}{\partial z}\right|_{z=h} = 0, \tag{5}$$

$$v_x|_{z=0} = -U. \tag{6}$$

The equations of motion integrate to

$$v_x = -U - \frac{3U}{2h^2}(z^2 - 2zh). \tag{7}$$

Since the loss of liquid by evaporation is low, we can as a first approximation set the loss to zero and use the condition of net zero volumetric flow rate, leading to Eq. (7). Eventually, we will calculate this term to show that it is small. In principle, an iterative procedure could also be used to relax the zero loss assumption. The equation for conservation of energy is

$$0 = k \frac{\partial^2 T}{\partial z^2} \tag{8}$$

subject to the conditions

$$T|_{z=0} = T_w, \tag{9}$$

$$T|_{z=h} = T_s. \tag{10}$$

The solution is

$$T = T_w - (T_w - T_s)\frac{z}{h}. \tag{11}$$

Substituting Eqs. (7) and (11) into Eq. (1) and integrating over z from $z=0$ to $z=h$, one has the integrand

$$\Phi = \frac{k\Delta T}{h} \ln \frac{T_w}{T_s} + \frac{3\mu U^2}{h}, \tag{12}$$

where $\Delta T = T_w - T_s$. Substituting $h = \alpha x$ and integrating over x from a microscale cutoff ℓ, to a macroscale cutoff L in Eq. (2), and rearranging, one has

$$\alpha^3 = 2 \ln\left|\frac{1}{\varepsilon}\right|\left[\frac{\mu k \Delta T/\gamma^2}{\mathrm{Ca}} \ln \frac{T_w}{T_s} + 3\mathrm{Ca}\right], \tag{13}$$

where $\varepsilon = \ell/L$ represents a very small quantity and Ca is the capillary number $\mu U/\gamma$, the ratio between viscous and surface tension forces. As the temperature of the vapor–liquid interface is a constant T_s, $N=0$ in Eq. (2). The singularity in ε represents a well-known feature in problems of dynamic contact lines.[13] The very weak logarithmic dependence on ε makes the lack of precise knowledge of ε relatively insignificant. When the viscous forces are important, the first term with square brackets in Eq. (13), which represents the heat transfer, becomes negligible and what is left is that $\alpha \propto \mathrm{Ca}^{1/3}$, or $\mathrm{Ca} \propto \alpha^3$ which is the familiar Hoffmann–Voinov–Tanner rule.[13] Joanny and de Gennes[7] first used the present method to obtain this result in the absence of heat-transfer effects. The nature of Eq. (13) is shown for some selected values of parameters in Fig. 2. As shown in Fig. 2, Eq. (13) admits only a minimum value of α,

$$\alpha_{\min}^3 = 4 \ln\left|\frac{1}{\varepsilon}\right|\left[\frac{3\mu k \Delta T}{\gamma^2} \ln \frac{T_w}{T_s}\right]^{1/2}, \tag{14}$$

which occurs at

$$U_{\min} = \left[\frac{k\Delta T}{3\mu} \ln \frac{T_w}{T_s}\right]^{1/2}. \tag{15}$$

The net loss of liquid volume by evaporation can be calculated as $(k\Delta T/\rho\lambda\alpha)\ln|1/\varepsilon|$ where ρ represents the liquid density and λ the latent heat of vaporization. Its ratio with U can be rewritten as the dimensionless $k/Uc\rho \cdot c\Delta T/\lambda \cdot 1/\alpha \cdot \ln|1/\varepsilon|$ where c is the specific heat. The first term is the ratio between conductive and convective heat transfer (inverse Peclet number) and is usually very small. The second term is the ratio between sensible heat and latent

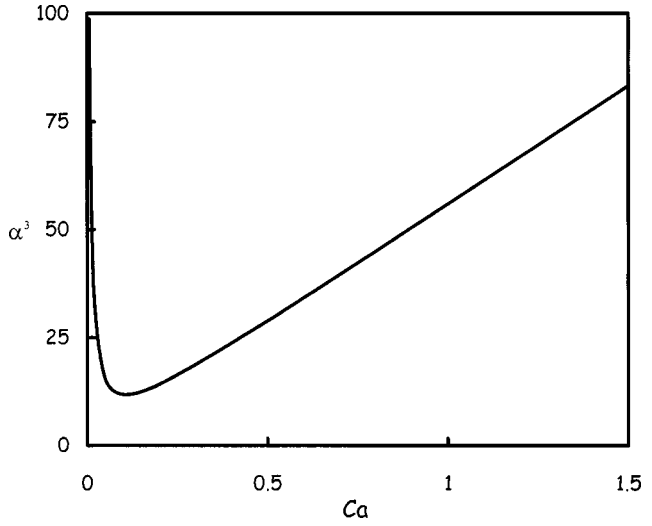

FIG. 2. α^3 plotted against Ca, for $\epsilon=10^{-4}$ from Eq. (13), $T_s=373$ K, and $T_w=383$ K. Other values used are $\gamma=72$ mN/m, $\mu=10^{-3}$ Pa·s and $k=0.68$ w/(mK), all appropriate for water at the normal boiling point.

heat and is very small. The last two terms are on the large side but within limits such that the overall dimensionless rate of loss of liquid volume remains small. No corrective iterative procedure to our zero loss approximation has been considered below.

Equation (13) possesses the appropriate asymmetry about heating and cooling. For the same magnitude of ΔT, α^3 is higher when $T_w<T_s$ than when $T_w>T_s$. This is understandable as condensation will thicken the film. The contact line advances in both cases of heating and cooling.

We note in passing that the present solution is valid only near the contact line and provides a boundary condition in the form of $\alpha(U)$. Normal stress balance must be analyzed to provide macroscopic quantities such as the height of the meniscus. The zero flow rate condition used to obtain Eq. (7) leads to a value for $\partial\wp/\partial x$. These quantities can be used to write a normal stress balance at the interface which includes the Laplace pressure to obtain a differential equation in profile h. A successive approximation scheme, which uses $h=\alpha x$ as a first approximation meniscus profile, can generate an updated profile. However, the existence of contact line singularity makes the problem quite difficult such that this straightforward procedure does not significantly improve the profile.

EVAPORATION INTO AIR

When air replaces the ambient fluid of saturated vapor in the last section, we must replace the saturation temperature T_s at the vapor–liquid interface with T_i which varies slowly with x. As a result, the surface tension γ also varies with x, and the Marangoni effect arises. In this case the boundary condition Eq. (5) becomes

$$\mu\left.\frac{\partial v_x}{\partial z}\right|_{z=h}=\frac{\partial\gamma}{\partial x}=\frac{\partial\gamma}{\partial T}\cdot\frac{\partial T_i}{\partial x} \tag{16}$$

leading to

$$\mu(v_x+U)=\frac{1}{2}\left(\frac{\partial\wp}{\partial x}\right)(z^2-2zh)+\beta\left(\frac{\partial T_i}{\partial x}\right)z \tag{17}$$

which at zero flow rate provides

$$\mu U=-\frac{h^2}{3}\left(\frac{\partial\wp}{\partial x}\right)+\frac{\beta h}{2}\left(\frac{\partial T_i}{\partial x}\right), \tag{18}$$

where $\beta=\partial\gamma/\partial T$ is as usual taken to be a negative quantity of constant value. The jump energy balance at the interface is

$$q_z=-k\frac{\partial T}{\partial z}=\lambda k_L p_{si}+\hat{h}(T_i-T_\infty), \tag{19}$$

where λ represents the latent heat, k_L the mass transfer coefficient, and $\hat{h}$ is the heat-transfer coefficient. Here p_{si} represents the saturation vapor pressure p_s, evaluated at the interfacial temperature T_i, and air far away at temperature T_∞ is assumed to be free of vapor. For small changes in T_i, the expansion

$$p_{si}=p_{sw}+\left(\frac{\partial p_s}{\partial T}\right)_w(T_i-T_w) \tag{20}$$

is used, where p_{sw} is p_s evaluated at the wall temperature T_w. We calculate T_i by noting that $\partial T/\partial z=(T_i-T_w)/h$, then using T as given in Eq. (11) except with T_i replacing T_s, and finally inserting Eq. (19) for the temperature gradient $\partial T/\partial z$ across the film, as

$$T_i=\frac{kT_w+h\left\{\hat{h}T_\infty-\lambda k_L\left[p_{sw}-\left(\frac{\partial p_s}{\partial T}\right)_w T_w\right]\right\}}{k+h\left[\lambda k_L\left(\frac{\partial p_s}{\partial T}\right)_w+\hat{h}\right]}. \tag{21}$$

Substituting for v_x, q_z, and T into Eq. (1) and integrating once from $z=0$ to $z=h$, one has

$$\Phi=\frac{k\hat{h}\Delta T}{h\hat{h}+k}\ln\frac{T_w}{T_i}+\frac{3\mu U^2}{h}+\frac{\beta^2 h}{4\mu}\left(\frac{\partial T_i}{\partial x}\right)^2, \tag{22}$$

where $\Delta T=T_w-T_\infty$. The integral of the first term contains a singularity at $x=\infty$. This contribution is subtracted off and integrated separately from $x=\ell$ to $x=L$, as done for Eq. (13). The remaining is integrated from $x=0$ to $x=\infty$. As before, the second term is integrated from $x=\ell$ to $x=L$, but no cutoffs are needed for the last term. That is, a cutoff is introduced only when there is a singularity. Following Eq. (2), the result is

$$\gamma\frac{\alpha^2}{2}U=-\frac{k\Delta T}{\alpha}[I(\delta)+I(\phi)]+\frac{k\Delta T}{\alpha}\ln\left\{\frac{\left[\hat{h}+\lambda k_L\left(\frac{\partial p_s}{\partial T}\right)_w\right]T_w}{\hat{h}T_\infty-\lambda k_L\left[p_{sw}-\left(\frac{\partial p_s}{\partial T}\right)_w T_w\right]}\right\}\ln\left|\frac{1}{\varepsilon}\right|+\frac{3\mu U^2}{\alpha}\ln\left|\frac{1}{\varepsilon}\right|$$
$$+\frac{\alpha^2\beta^2[\lambda k_L p_{sw}+\hat{h}\Delta T]^2}{24\mu\left[\lambda k_L\left(\frac{\partial p_s}{\partial T}\right)_w+\hat{h}\right]^2}+\frac{U\beta}{2}\frac{\hat{h}\Delta T+\lambda k_L p_{sw}}{\hat{h}+\lambda k_L\left(\frac{\partial p_s}{\partial T}\right)_w}, \tag{23}$$

where

$$I(\omega)=\int_0^1\frac{\ln(1+\omega Y)}{Y}dY=\omega-\omega^2/2^2+\omega^3/3^2-\cdots$$

and

$$\delta=\frac{\hat{h}\Delta T+\lambda k_L\left[p_{sw}-\left(\frac{\partial p_s}{\partial T}\right)_w T_w\right]}{\hat{h}T_\infty-\lambda k_L\left[p_{sw}-\left(\frac{\partial p_s}{\partial T}\right)_w T_w\right]}$$

and

$$\varphi=\frac{\lambda k_L\left(\frac{\partial p_s}{\partial T}\right)_w}{\hat{h}+\lambda k_L\left(\frac{\partial p_s}{\partial T}\right)_w}.$$

Note that Eq. (23) has a dependence on α that is similar to the previous problem, Eq. (13) and Fig. 2.

The last term on the right-hand side in Eq. (23) is the term N in Eq. (2). It has been calculated using the following procedure. At the liquid–air interface, $-\gamma_\infty\cdot v_x|_{z=h}$ ($x=\infty$ where $h=\infty$) is the rate of surface work done at one end, and $\gamma v_x|_{z=h}$ ($x=0$ where $h=0$) is the rate of surface work done at the other end. Then the energy that has to be supplied to the system is $(\gamma-\gamma_\infty)(U/2)$ where both the velocities in above are calculated to be $U/2$ using Eqs. (17), (18), and (21). In addition, γ_∞ is the surface tension calculated at temperature $T_i(x=\infty)$, the bulk value, and γ is that calculated at $T_i(x=0)$, the value at the contact line. This term can be further simplified as $(\partial\gamma/\partial T)[T_{i,x=0}-T_{i,x=\infty}](U/2)$, which becomes the last term in Eq. (23). The present procedure to calculate N appears to be fairly general and should work for most boundary value problems.

Liquids such as silicone oils are nonvolatile, a case which is reached here when k_L approaches zero,

$$U\gamma\frac{\alpha^2}{2}=-\frac{k\Delta T}{\alpha}I(\chi)+\frac{k\Delta T}{\alpha}\ln\frac{T_w}{T_\infty}\ln\left|\frac{1}{\varepsilon}\right|+\frac{3\mu U^2}{\alpha}\ln\left|\frac{1}{\varepsilon}\right|$$
$$+\frac{\alpha^2\beta^2(\Delta T)^2}{24\mu}+\frac{U\beta}{2}\Delta T, \tag{24}$$

where $\chi=\Delta T/T_\infty$.

We can also look at evaporative systems with no external heating, in which case $\Delta T=0$, and Eq. (23) becomes

$$\gamma\frac{\alpha^2}{2}U=\frac{3\mu U^2}{\alpha}\ln\left|\frac{1}{\varepsilon}\right|+\frac{\alpha^2\beta^2[\lambda k_L p_{sw}]^2}{24\mu\left[\lambda k_L\left(\frac{\partial p_s}{\partial T}\right)_w+\hat{h}\right]^2}$$
$$+\frac{U\beta}{2}\frac{\lambda k_L p_{sw}}{\hat{h}+\lambda k_L\left(\frac{\partial p_s}{\partial T}\right)_w}. \tag{25}$$

As expected, the Marangoni effect remains, and the interfacial temperature T_i decreases away from the contact line.

RESULTS AND DISCUSSION

The situations shown in Fig. 1 and analyzed earlier are of forced spreading where U is an independent variable. The special case of spontaneous spreading, where the plate is held stationary and the meniscus climbs upwards, is obtained by setting $U=-dx_0/dt$ where $x_0(t)$ is the position of contact line.

As in the case where the ambient fluid is a saturated vapor, Eq. (13), the case where the ambient fluid is air, Eq. (23), also shows asymmetry with respect to heating and cooling. This can be seen from the first two terms on the right-hand side of Eq. (23). Of these, the analog of the first term does not exist in Eq. (13). It is a term that is fully asymmetric, negative for heating and positive for cooling. Consequently, the contact angle decreases on evaporation since the films are thinned, and increases on condensation since the films are thickened.

If the last term in Eq. (23) is ignored, the equation can be expressed more compactly as

$$\alpha^3\mathrm{Ca}=a+b\mathrm{Ca}^2+c\alpha^3 \tag{26}$$

or

$$\alpha=\left[\frac{a+b\mathrm{Ca}^2}{\mathrm{Ca}-c}\right]^{1/3}, \tag{27}$$

where a, b, and c are constants, where at least b and c are positive. At large Ca, α becomes proportional to $\mathrm{Ca}^{1/3}$. Morris[7] used the results of Kim[14] and Kim and Wayner[15] to calculate α as a function of Ca as shown in Fig. 3. These experiments were conducted under air and hence the Marangoni effect will always exist, although its relative importance may vary. Figure 3 shows that Eq. (27) fits octane data very well, but it is statistically only a little better than Morris' result after accounting for the fact that we have two param-

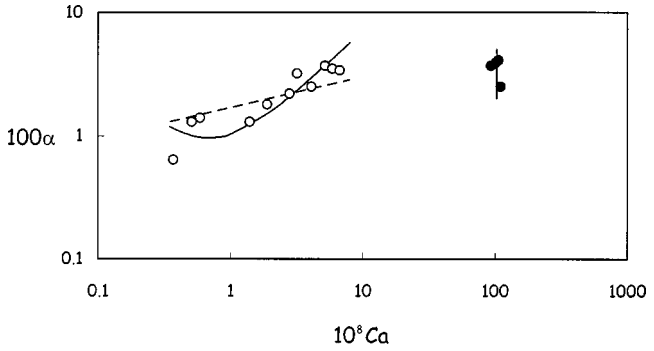

FIG. 3. The data for octane (open circles) and R113 (closed circles) from Kim (Ref. 11) and Kim and Wayner (Ref. 12), as described by Morris (Ref. 7) are shown along with the theoretical predictions. The curve in bold is Eq. (26) fitted to octane data for $c=0$. That is, Morris's result which has no Marangoni effect, is being compared to the present results with no Marangoni effect. Calculated values are $a=9.83\times10^{-15}$ and $b=210.8$. The dashed line is Morris's result for $\alpha=1.697\,\mathrm{Ca}^{1/4}$. All parameters were estimated using weighted nonlinear regression with inverse values as weights. For such estimates, the residual sum of squares per degree of freedom was only slightly better in the present work over Morris's. That is, the fact that Morris has one parameter and we have two was included. The bold line passing through the data for R113 is Eq. (28) where $\mathrm{Ca}=c$ is determined as 102.5.

eters compared to one for Morris. Here c, which represents the Marangoni effect, was set to zero to comply with the results of Morris who has ignored the Marangoni effect.

In contrast to the octane data, we attribute the behavior of data on R113, fluorinated hydrocarbon, to a large Marangoni effect. Neglecting all but the last term on the right-hand side in Eq. (26), we find that α does not depend on Ca or that $\mathrm{Ca}=c$. This independence on Ca adequately describes the experiments on R113 as shown in Fig. 3. The critical capillary number is

$$c=\frac{\beta^2[\lambda k_L p_{sw}+\hat{h}\Delta T]^2}{12\gamma^2\left[\lambda k_L\left(\frac{\partial p_s}{\partial T}\right)_w+\hat{h}\right]^2}. \tag{28}$$

For one fluorinated hydrocarbon,[16] data indicate a magnitude of c of 3.5×10^{-5} for $\Delta T=5$ K and under the assumption that latent heat is negligible. It is seen to be 10^{-6} in Fig. 3. If the latent heat is significant, the values of c would be lower because of the fast increase of vapor pressure with temperature.

Bascom *et al.*[8] conducted experiments in a system where a volatile impurity was present and allowed to evaporate. It can be assumed in those cases that the contact line region is stripped of the volatiles. In one case, this contact line region has a lower surface tension than the interior and hence the Marangoni force is pointed from the contact line towards the interior. This case mimics a heating situation where as the substrate temperature is higher than the interfacial temperature T_i, and T_i decreases away from the region near the contact line. Hence the Marangoni force in this case is also directed away from the region near the contact line. The reverse case was also studied by Bascom *et al.*,[8] and represents an analog of cooling. Experimentally, Bascom *et al.* found that the ''heating'' case has a lower contact angle than the ''cooling'' case (see also Neogi[17]). To compare these results to the present findings, consider the case of evaporation, Eq. (24). In addition, the temperature differences are assumed small such that terms of order $(\Delta T)^2$ (first, second, and fourth terms) on the right-hand side can be neglected. The fifth term, which has been neglected so far, becomes important here as it provides the asymmetry to heat and cooling. It increases the right-hand side, hence α, on cooling and decreases α on heating (recall that β is negative).

Renk and Wayner[5] conducted a different experiment in which the film profile is initially isothermal and has a very small value of α. The heaters are then turned on and set to a value of T_w at the plate. Both cases studied show that there is a minimum $\alpha_{\min}$. Consequently, starting with a value of α less than this minimum, some form of disturbance is expected to be seen (''kicking and biting motions'') until the minimum is exceeded. This observation has been reported by Renk and Wayner[5] to occur in some instances before the meniscus settles down.

The main basis for expecting instability in the system studied here is that for a large Marangoni effect, α is predicted to be unconstrained, that is the contour of the contact line has no constraints. In their experiments on spreading at a large Marangoni force induced by concentration gradients, Cottington *et al.*[18] observed that the contact line moved with turbulence and often burst with some violence, confirming our expectations. Less dramatic events are reported elsewhere.[3,4] It is not possible to consider all these cases without a detailed stability analysis.

It appears from the present analysis the method given by Joanny and de Gennes[7] is very easy to apply. In contrast, the conventional transport phenomena give rise both to mathematically complex problems as well as limit solutions to restricted values of parameters.[6,19] Wayner and co-workers[5,14,15] suggest that their experiments could also be represented by a constant flux boundary condition at the wall instead of the constant temperature boundary condition used here. In this case we failed to get satisfactory results since the contact angle was seen to depend strongly on the macroscale L.

ACKNOWLEDGMENT

This material is based on work supported by the National Science Foundation under Grant No. CTS-0228834.

[1] V. K. Dhir, AIChE J. **47**, 813 (2001).
[2] W. M. Rohsenow, in *Developments in Heat Transfer*, edited by W. M. Roshenow (M.I.T., Cambridge, MA, 1964), p. 169.
[3] A. M. Cazabat, F. Heslot, S. M. Troian, and P. Carles, Nature (London) **346**, 824 (1990).
[4] O. Benichou, M. Cachile, A. M. Cazabat, C. Poulard, M. P. Valignat, F. Vandenbrouck, and D. van Effenterre, Adv. Colloid Interface Sci. **100–102**, 381 (2003).
[5] F. J. Renk and P. C. Wayner, Jr., J. Heat Transfer **101**, 59 (1979).
[6] S. J. S. Morris, J. Fluid Mech. **432**, 1 (2001).
[7] J. F. Joanny and P. G. de Gennes, C. R. Acad. Sci., Ser. II: Mec., Phys., Chim., Sci. Terre Univers **299**, 279 (1984).
[8] W. D. Bascom, R. L. Cottington, and C. R. Singleterry, *Contact Angle, Wettability and Adhesion*, Adv. Chem. Ser. No. 43 (Am. Chem. Soc., Washington, DC, 1964), p. 335.
[9] M. M. Denn, *Process Fluid Mechanics* (Prentice-Hall, Englewood Cliffs, NJ, 1980), p. 265.
[10] S. R. de Groot and R. Mazur, *Non-Equilibrium Thermodynamics* (North-

Holland, Amsterdam, 1962, reprinted by Dover, New York), p. 20.
[11] M. E. R. Shanahan, Langmuir **17**, 3997 (2001).
[12] M. E. R. Shanahan, Langmuir **17**, 8229 (2001).
[13] S. F. Kistler, in *Wettability*, edited by J. C. Berg (Dekker, New York, 1993), p. 311.
[14] I. Y. Kim, Ph.D. thesis, Rensselaer Polytechnic Institute, Troy, NY, 1994.
[15] I. Y. Kim and P. C. Wayner, Jr., J. Thermophys. Heat Transfer **10**, 320 (1996).
[16] A. W. Adamson, *Physical Chemistry of Surfaces*, 5th ed. (Wiley Interscience, New York, 1990), p. 57.
[17] P. Neogi, J. Colloid Interface Sci. **105**, 94 (1985).
[18] R. L. Cottington, C. M. Murphy, and C. R. Singleterry, in *Contact Angle, Wettability, and Adhesion* (Ref. 8), p. 341.
[19] S. J. S. Morris, J. Fluid Mech. **411**, 59 (2000).